# EIS microfluidic chips for flow immunoassay and ultrasensitive cholera toxin detection

**Maria Serena Chiriacò,*[ab] Elisabetta Primiceri,[ab] Eliana D'Amone,[a] Rodica Elena Ionescu,†[b] Ross Rinaldi[ac] and Giuseppe Maruccio*[ad]**

*Received 14th September 2010, Accepted 29th October 2010*
**DOI: 10.1039/c0lc00409j**

A flow-injection impedimetric immunosensor for the sensitive, direct and label-free detection of cholera toxin is reported. A limit of detection smaller than 10 pM was achieved, a value thousands of times lower than the lethal dose. The developed chips fulfil the requirement of low cost and quick reply of the assay and are expected to enable field screening, prompt diagnosis and medical intervention without the need of specialized personnel and expensive equipment, a perspective of special relevance for use in developing countries. Since the chip layout includes two sensing areas each one with a 2 × 2 sensor array, our biochips can allow statistical or (alternatively) multiplex analysis of biorecognition events between antibodies immobilized on each working electrode and different antigens flowing into the chamber.

## Introduction

In recent years, miniaturization of biosensors and their integration in microarrays and functional biochips enabled massive parallel detection of analytes, diseases and disease susceptibilities, as well as identification of personalized drug response profiles. Examples of bioassays and biological procedures that have been miniaturized into a chip format include DNA sequencing, polymerase chain reaction, electrophoresis, DNA separation, enzymatic assays, immunoassays, cell counting, cell sorting, cell culture, and high-throughput screening in drug development. In all these applications, the microfluidic approach brought new opportunities and capabilities. These progresses opened the way to novel devices and biochips which allow analyzing in parallel large numbers of biological molecules, cells and drugs.[1–7] Another recent promising application concerns the detection of biological pathogens and disease-associated markers.[8]

Cholera toxin is an enterotoxin of *Vibrio cholerae*, composed of two subunits, A (27 kDa) and B (11.6 kDa), arranged in hetero-hexameric structures of type AB5.[9] The B subunit known as a "*choleragenoid*", binds to the natural receptors (GM1 gangliosides) on the epithelial cell membrane of the small intestine, particularly the jejunum and duodenum. In the subsequent cascade reaction, the fragment A1 of the A subunit is translocated through the membrane of the host cells, triggering endocytosis,[10] activating the adenylate cyclase and causing a strong efflux of ions and water from the infected cells, leading to the appearance of first cholera symptoms: the painless and copious rice-water diarrhea, up to 20 l in 24 h.[11] This diarrhea is later joined by vomiting, causing severe dehydration and can be lethal in 3–4 hours for untreated patients.[12,13] As highlighted by the World Health Organization,[14] cholera is a major threat to human health that periodically spreads worldwide in pandemic waves from its endemic area in South-East Asia. It is becoming increasingly important as the number of countries affected continues to increase and new major outbreaks to occur worldwide, especially in the wake of climate changes or where living conditions are crowded and water sources unprotected. To give an idea of the associated risk, in 1994 in a refugee camp in Goma, Democratic Republic of the Congo, a major epidemic took place, leading within only one month to 58 000–80 000 estimated cases and 23 800 deaths.[14] The lethal dose for cholera toxin in human is relatively low ($LD_{50} \approx 250\ \mu g\ kg^{-1}$), but rapid medical treatment including carbohydrates/electrolytes solutions and antibiotics[15] can avoid death. So, there is a clinical need for the development of accurate, simple and rapid methods for detecting the bacterially secreted toxin with high sensitivity. In particular, field use without the need of skilled operators is of extreme importance for developing countries.

Conventional methods for detection mainly address the cholera toxin subunit B (CT) and are based on recognition between cholera toxin and either gangliosides or specific antibodies. In the first case, most of the reported methodologies employ the receptor ganglioside GM1 immobilized on the sensing area[16] or incorporated into lipid membranes/liposomes functionalized with fluorescent labels (*e.g.* horseradish peroxidase or sulforhodamine).[13,17–20] Recently the specific binding of cholera toxin B-oligomer to the GM1 ganglioside embedded in lipid-membrane segments of 1,2-dimyristoyl-*sn*-*glycero*-3-phosphocholine was investigated by scanning force microscopy.[21] Within the second approach,[22–28] specific antibodies were employed in microarrays for the detection of native toxins in solution but their use often required the presence of secondary fluorescently labelled antibodies in a sandwich type screening or a competitive assay between a labelled toxin and the unlabeled

[a]*NNL CNR-Istituto di Nanoscienze, Via per Arnesano, Lecce, Italy. E-mail: serena.chiriaco@unisalento.it; giuseppe.maruccio@unisalento.it*
[b]*Scuola Superiore ISUFI, Univ. of Salento, Via per Arnesano, Lecce, Italy*
[c]*Dept. of Innovation Engineering, University of Salento, Via per Arnesano, Lecce, Italy*
[d]*Dept. of Physics, University of Salento, Via per Arnesano, Lecce, Italy*
† Current address: Laboratoire de Nanotechnologie et d'Instrumentation Optique, Institut Charles Delaunay, Université de technologie de Troyes, UMR STMR CNRS 6279, 12 rue Marie-Curie BP2060 10010 TROYES, Cedex, France.

one to be detected.[23,24] Beyond fluorescence[16,18,19] and chemiluminescence,[17] other label-free detection methods involved the use of nanoparticles for colorimetric detection[29,30] and the conjugation of the antibodies to gold nanoparticles was reported to result in an improved sensitivity due to the increase in the ligand density on the sensing surface.[30,31] Among immunosensors based on antigen–antibody interactions, electrochemical transducers are the most interesting and electrochemical impedance spectroscopy (EIS) has been applied for label-free detection of cholera toxin by monitoring the electrical properties of electrode surfaces modified with a redox biotinylated poly(pyrrole-viologen) electrogenerated film.[32] The use of carbon nanotubes to increase the sensitivity was also reported.[33] Moreover, surface plasmon resonance (SPR) and impedance measurements on ion-sensitive field-effect transistors were used as well and compared for signal transduction.[22] In few cases, microfluidic components for automatic sample handling were integrated with the biosensors resulting in great advantages in terms of costs, speed and easiness of use.[18] For example, flow-injection capacitive immunosensors for cholera toxin were reported based on SPR transducers employing self-assembled monolayers of antibodies immobilized on a gold surface.[26]

Here we report the development of label-free EIS immunosensors enabling a highly sensitive detection of CT down to 1 ng $ml^{-1}$. Compared to literature, the integrated microfluidic platform for sample handling allows us to exploit the advantages of flow immunoassays in terms of quantitative results, speed, reduced sample handling and cost. Neither fluorescent tagging of reagents nor complex instrumentation and/or skilled operators are necessary. Our biochips include two reaction chambers with eight sensing areas for statistical analysis and monitor the biorecognition events between antibodies immobilized on gold electrodes surface and B subunit of cholera toxin flowing into the chamber. The use of CT antibodies instead of GM1 ganglioside receptors was dictated by consideration of the typical location of cholera outbreaks and the target of field use, in which case the GM1 ganglioside stability presents a concern as the sialic acid (Neu5Ac) glycosidic linkage is labile.[29]

## Experimental section

### Materials and chemicals

Glass substrates (2.5 cm × 2.5 cm) were purchased from Visionteck. SU-8 resist was obtained from Microchem, AZ resist from Clariant and the polydimethylsiloxane (PDMS) kit from *Sylgard 184*. β-Mercaptoethanol, 11-mercaptoundecanoic acid (MUA), *N*-hydroxysuccinimide (NHS) and *N*-ethyl-*N*′-(3-dimethylaminopropyl)carbodiimide hydrochloride (EDC) were obtained from *Sigma Aldrich*. Protein A from *Staphylococcus Aureus*, bovine serum albumin (BSA), anti-cholera toxin antibodies (Ab) and B subunit of cholera toxin were also purchased at the maximum degree of purity from *Sigma Aldrich*.

### Fabrication and assembly of the microfluidic chip

Gold interdigitated electrodes (with 10 μm spacing and width) were fabricated on glass substrates by optical lithography using a Karl Suss MJB3 mask aligner and AZ5214B resist. Each device consists of two sensing areas, both including four interdigitated electrodes to allow statistical analysis or microarray detection (Fig. 1). Microfluidic chambers with their own inlet and outlet microchannels were fabricated by replica molding from a hard master made by a 200 μm height SU-8 photoresist. A ratio of 10 : 1 PDMS/curing agent solution was used for the replica. To assemble the whole device a step of oxygen plasma exposure of PDMS (20 minutes at 0.5 mbar) and a rapid cleaning of the glass with the electrodes in piranha solution were carried out. Such microfluidic chips were already demonstrated to be able to monitor the toxicity of copper ions on cultured cells by impedance measurements.[7]

### Surface functionalization of the device

To implement microfluidic chips able to detect CT in the aqueous solution flowing into the sensing chamber, our strategy consisted in the immobilization of anti-cholera toxin antibodies on gold electrodes (Fig. 2a). The first step for this functionalization was an overnight deposition of a mixed SAM of 11-mercaptoundecanoic acid (MUA) and 2-mercaptoethanol (2-ME) in a ratio of 1 : 5 (0.2 mM of MUA and 1mM of 2-ME). After monolayer formation, electrodes were rinsed in ethanol to remove any physisorbed thiol and washed in milliQ water. Then, a step of activation of the COOH groups is required. This was achieved by means of an incubation with *N*-hydroxysuccinimide (NHS) and *N*-ethyl-*N*′-(3-dimethylaminopropyl)carbodiimide hydrochloride (EDC) in a ratio of 1 : 4 in milliQ water for 30 minutes to form reactive *N*-hydroxysuccinimide esters. Following the functionalization, the electrodes were incubated in a solution with protein A for 2 h in PBS (phosphate buffer solution), which bond covalently on the substrate *via* their N termini protein residues by replacing NHS groups in the layer. Then excess esters were deactivated in ethanolamine 1 M in water and the samples were incubated in a BSA 10 mg $ml^{-1}$ solution for about 1 h to saturate the unbounded sites of the electrode and to make homogeneous the new surface that will hold the antibodies. This is possible because the structure of protein A is naturally

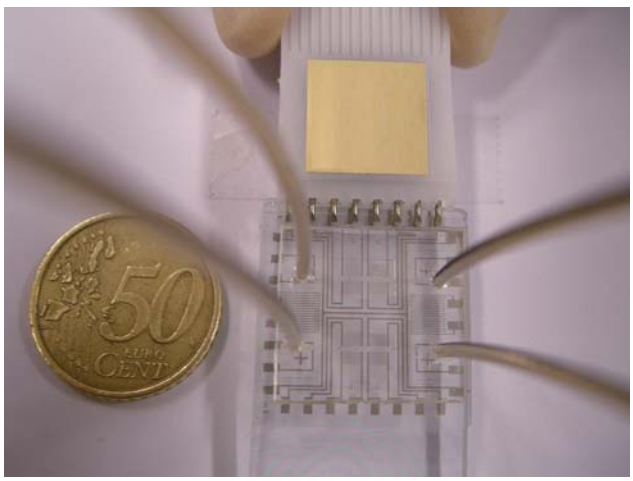


**Fig. 1** Biochip layout. Interdigitated electrodes, temperature sensors and heaters are made of gold on glass substrate. PDMS microfluidic components are assembled on the substrate and include chambers with microchannels, inlet and outlet tubes.

 

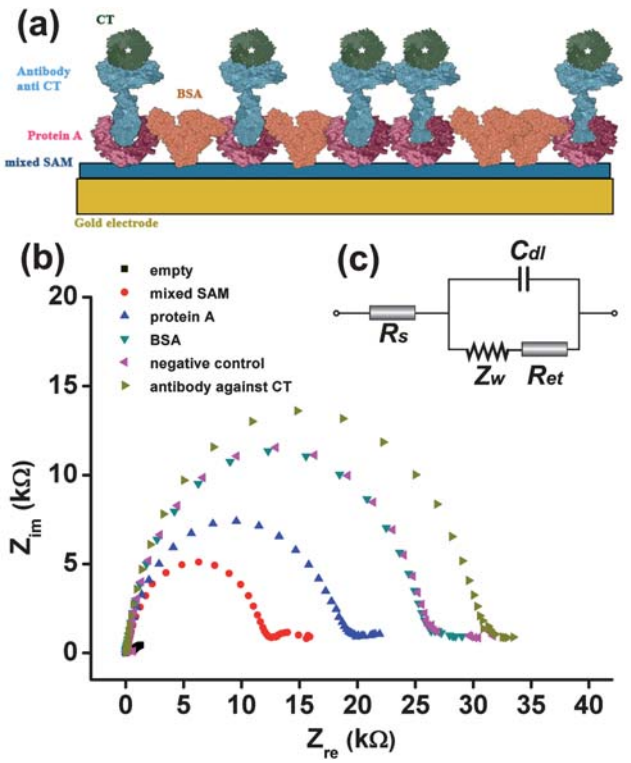


**Fig. 2** (a) Schematic representation of electrode functionalization. (b) Nyquist spectra corresponding to the different functionalization steps. After each step, an increasing in impedance values is observed, except in the case of the negative control (cyan curve). (c) Equivalent circuit for impedance spectroscopy measurements. The circuit includes ohmic resistance of the electrolyte solution $R_s$, Warburg impedance $Z_w$ resulted from the ionic diffusion of the electrolyte, double layer capacitance $C_{dl}$ and electron transfer resistance $R_{et}$.

customized to hold the Fc portion of Ab. Anti-cholera toxin antibodies are then immobilized onto the functionalized area incubating in a solution diluted 1 : 2000 with respect to the concentration of the product as purchased. Such functionalized electrodes were then employed to detect CT in the flowing solution at decreasing concentration (from 100 ng ml$^{-1}$ to 1 ng ml$^{-1}$) to establish the detection limit of our impedimetric chips.

### Impedance measurements

Impedance measurements were performed in the frequency range between 0.1 and $10^6$ Hz using an impedance analyzer (Autolab PGSTAT30, Eco Chemie) and a sinusoidal ac voltage with a 15 mV RMS amplitude. To fully characterize our device response, for each step of functionalization the solution present in the chamber was replaced with a solution of PBS added with a redox couple of potassium hexacyanoferrate(II/III) $K_3[Fe(CN)_6]$/$K_4[Fe(CN)_6]$ (1 : 1) (Sigma Aldrich) at a final concentration of 10 mM and then the measurements were performed. Specifically, impedance curves were acquired from as-fabricated devices and after adsorption of mixed SAM of MUA/2-ME 1 : 5, Protein A deposition, BSA homogenization and antibody functionalization. Due to the described layout consisting of two sensing chambers, each of them with its own inlet/outlet microfluidic channels and including four couples of interdigitated electrodes, it was possible to make four measurements for each chamber, so that with a single injection of the sample we have significant information about reproducibility of the impedance measurements by maintaining the identical conditions of functionalization of each electrode. To obtain the calibration dose–response curve for CT detection, we made parallel experiments employing several devices which were simultaneously functionalized to assure the same conditions for each point of concentration tested (statistical variations from different devices in the same conditions are small and negligible in this respect).

## Results and discussion

### Device functionalization and optimization

Impedance spectroscopy is very effective for detecting bio-recognition events on surface-modified electrodes.[34,35] When AC impedance spectra are plotted in the form of Nyquist diagrams ($Z_{im}$ as a function of $Z_{re}$, with frequency increasing from right to left), two regions typical of a reversible reaction at solid interface can be distinguished. The portion with semicircle shape obtained at high frequencies corresponds to faradic electron-transfer at the electrodes, while the spectrum obtained for low frequencies gives information about the diffusion process of transport of the redox species in the electrolyte to the electrode surface. The characteristic frequencies for diffusion fall into the range of 1–10 Hz, while the electron transfer kinetics and double layer effects are more important at higher frequencies. The corresponding frequency range for most electrochemical reactions is from 100 to 1000 Hz.[36] The time constant for double layer charging corresponds to a frequency region >10 kHz. The information of interest about the surface chemistry can be derived by modelling the charge flow with an equivalent (Randles) circuit (Fig. 2c), where the interfacial layer at the working electrode is represented by an electron transfer resistance $R_{et}$ in parallel combination with a capacitance $C_{dl}$ accounting for the electrical double layer at the interface, and a series Warburg impedance $Z_w$ describing depletion of the redox species at the interface. Additionally a series resistance $R_s$ accounts for the uncompensated solution resistance.[34] $R_{et}$ is very sensitive to electrode modifications, allowing detection of bio-recognition events with high sensitivity.

In Fig. 2b, the evolution of the impedance spectra with the different functionalization steps is reported. As expected, each additional layer (Fig. 2b) on the electrodes clearly leads to an impedance increase. Specifically, the bare gold electrode (black curve) shows a very small semicircle region, corresponding to a very low electron transfer resistance $R_{et}$ (Fig. 2b). This is the starting point for the fabrication of our biochip and the following functionalization was optimized in order to have an ideal surface chemistry suitable for CT detection with high selectivity and sensitivity. In this respect, we found that in the first functionalization step the deposition of a mixed self-assembled monolayer (SAM) of 11-mercaptoundecanoic acid (MUA) and β-mercaptoethanol (2-ME) with a ratio of 1 : 5 leads to better results as compared to similar devices where a monolayer consisting of only mercaptoundecanoic acid molecules is present. The reason is that such molecules alone tend to form dense and ordered monolayers that exhibit higher impedance and thus reduce sensitivity affecting the detection limit of toxin. On the other

hand, in the case of mixed SAMs, the 2-ME molecules act as spacers in the monolayer and improve charge transfer at the working electrodes due to their smaller dimensions (red curve in Fig. 2b). Additionally, a reduction of MUA coverage in the monolayer leads to another advantage: proteins required for the following steps attach the surface of the mixed SAM to the carboxylic end of MUA and the increased spacing between two neighbour molecules of MUA avoids steric problems in the homogeneous deposition of proteins and their ability to act as recognition probes.[37,38] Then, in the following functionalization step, a layer of Protein A from *S. Aureus* was covalently immobilized onto the mixed-SAM-modified electrodes (blue curve in Fig. 2b), which were subsequently incubated with BSA (cyan curve in Fig. 2b) to make the surface homogeneous and to saturate unspecific sites before depositing antibodies against CT. Antibody molecules bind Protein A with their portion Fc, exposing their specific Fab portion which is thus available for recognition of CT in solution (yellow curve in Fig. 2b).

In order to verify the specificity expected from recognition between CT and its antibody, we performed dedicated control experiments. Specifically, devices prepared without antibody deposition were directly incubated (after BSA immobilization) in a solution with CT at the highest concentration (100 ng ml$^{-1}$) used in the calibration experiments. As clearly shown in Fig. 2b, in this case, the corresponding pink curve is quite overlapped to the curve obtained after BSA deposition. Thus, we conclude that CT binds only to its specific antibody with negligible interaction with the other layers. Notably, after all the functionalization steps, impedance values are still low (around 30 kΩ), thus allowing high sensitivity, as described in the next section.

### Calibration of the chip for CT detection

Once anti-cholera toxin antibodies are immobilized, CT molecules can be easily detected and we evaluated the sensitivity of our chips by incubating modified electrodes with aqueous sample containing a decreasing amount of CT, ranging from 100 ng ml$^{-1}$ to 1 ng ml$^{-1}$. When captured from solution on the electrode surface by the immobilized antibodies, the toxins modulate the rate of electron transfer between redox probes in the medium and the working electrodes, depending on their bulkiness and charges. The result is a measurable increase in charge transfer resistance $R_{et}$. As shown in Fig. 3, a regular decrease in impedance values and the related diameter of the Nyquist plot with lower CT concentrations was observed.

Fig. 4 displays the dose–response calibration curve obtained by plotting the electron transfer resistance $R_{et}$ with its standard deviation (SD) as a function of the CT concentration tested. The dynamic range covered all the investigated concentrations and was at least from 1 ng ml$^{-1}$ to 100 ng ml$^{-1}$, with some deviation from linearity at higher concentrations that can be easily compensated with a computer-assisted reading. Such deviations probably indicate that we are approaching saturation of the specific binding sites in a concentration between 75 and 100 ng ml$^{-1}$. The lowest concentration detected was as low as 1 ng ml$^{-1}$ corresponding to $1.2 \times 10^{-11}$ M. However, the limit of detection estimated as three SD above the background is smaller: $0.5 \times 10^{-11}$ M. Flow immunoassays performed on the four couples of electrodes in each sensor chamber demonstrated an average

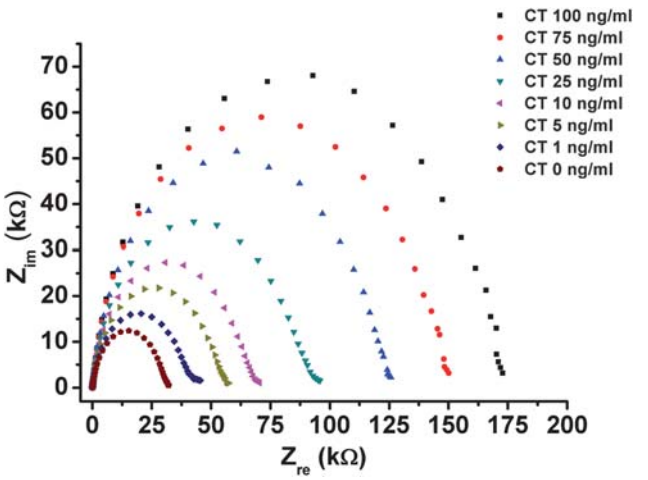


**Fig. 3** Nyquist spectra acquired during dose–response calibration and corresponding to detection of different CT concentrations.

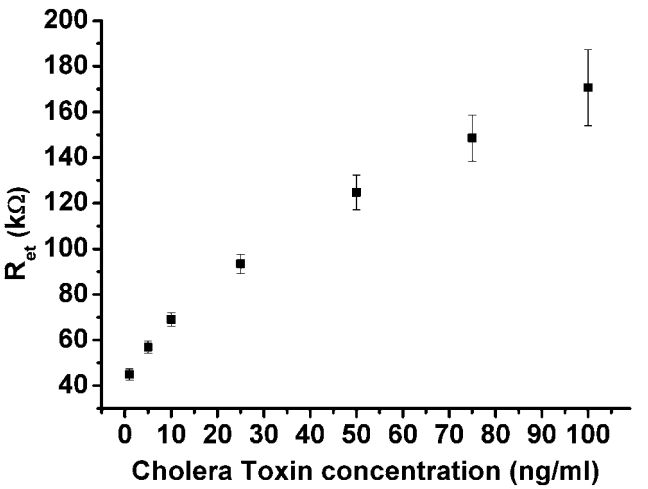


**Fig. 4** Electrical transfer resistance values as a function of CT concentration.

variation of about 3% in the $R_{et}$ values at each concentration tested but similar calibration curves and limit of detection were obtained. As far as functionalization and analysis times are concerned, all the steps for antibody immobilization and injection of the sample were made in sequence using the PDMS microchannels. This leads to a low diagnosis time, mainly corresponding to the time for the biorecognition event (1 hour) since impedance measurements take only 5 minutes. This time can be further reduced by monitoring in real time the impedance at a selected frequency since this would allow to follow the transient during biorecognition and calibrate the response curve at a small delay time after sample injection.

As compared to previously published methods (Table 1), our chip represents a competitive diagnostic tool for CT detection, because of a unique combination of sensitivity (1 ng ml$^{-1}$, smaller or comparable to most of the methods proposed in literature) and response time. We emphasize that the few reports where the LOD is lower than in our biochips either calculated the LOD values from the signal to noise ratio or made use of special

 

**Table 1** Comparison with literature

| Bibliographic reference | LOD/pM | Sensing element | Transduction | Fluidics |
|---|---|---|---|---|
| *Our biochip* | *12* | *Ab immobilized on gold microelectrodes* | *Electrochemical impedance* | *Yes* |
| (3SD=) | 5 | | | |
| 29 | 54 000 | Lactose derivative | Colorimetric (with NP) | No |
| 40 (entire toxin, not subunits) | 10 000 | GM1 | Cyclic voltammetry | No |
| 22 | 1200 | Ab | SPR and ISFET | No |
| 41 | 1200 | Monosaccharides | Fluorescence | No |
| 18 | 210 | GM1 | Fluorescence | No |
| 27 | 120 | Ab | Fluorescence | Multiple |
| 25 | 95 | Ab | Fluorescence | Multiple |
| (3SD=) | 3.6 | | | |
| 19 | 50 | GM1 | Fluorescence quenching and/or resonant energy transfer | No |
| *Commercial kit (working with bacterial cells)* | *20* | *Ab on polystyrene latex particles* | *Optical* | *No* |
| 13 | 12 | Both | Fluorescence and electrochemistry | Yes |
| 28 | 12 | Ab on hydrogel | Fluorescence | No |
| 20 | 4.8 (=3SD) | GM1 | Fluorescence | No |
| 26 | 0.1 | Ab | Capacitive | No |
| (3SD=) | 0.01 | | | |
| 17 | 0.01 (=3SD) | GM1 + Ab | Chemiluminescence | No |
| 33 | 0.0001 | GM1 + Ab | Electrochemistry (using CNT) | No |
| 12 | 0.0001 | GM1 + Ab | Colorimetric | No |

materials and procedures (like carbon nanotubes or immunomagnetic separation) which increase sensitivity but also costs. In our biochips, the presence of fluidic components facilitates and speeds up the functionalization of the transducer, reducing also the reagent costs due to the very small volumes required. The fabrication cost of our prototypes in the lab is estimated to be around 3 € per unit and is already competitive although a significant decrease can be certainly obtained at the industrial level.

## Conclusions

In conclusion we reported the combination of flow immunoassay and EIS for increased detection sensitivity, automated sample handling in small volumes, shorter assay times and field use. An optimization of the functionalization and a completely label-free EIS transduction allowed detection of 1 ng $ml^{-1}$ of CT. This value is more than a thousand of times smaller than the lethal dose and results in a really competitive tool both with commercial kits and other biosensing technologies in literature. Standard tests for the detection of CT include the GM1 technique and antibodies immobilization on standard plates for ELISA screening. These methods allow a sensitive detection of the toxin but they are expensive and time consuming both for preparation of the platform required for analysis and for measurements. Moreover they often use fluorescent labelling as a tool for detection and so technology costs increase. The developed chips instead, fulfil the requirement of low cost and quick reply of the assay. Moreover, they represent an important step towards portability, since the fluids to be analyzed can be introduced by a simple syringe while the impedance analyzer could be reduced to an electronic board integrated/connected to a laptop and enabling impedance measurements at a selected output frequency. Thus they could enable field screening, prompt diagnosis and medical intervention without the need of specialized personnel and expensive equipment, a perspective of special relevance for use in developing countries, where the need is more urgent and clinical laboratories are totally rare or absent. The presented biochip represents a very attractive alternative to the existing methods due to simplicity, high sensitivity and inexpensive instrumentation. Since the chip layout includes two sensing areas each one with $2 \times 2$ array sensor, our biochips can allow statistical or (alternatively) multiplex analysis of biorecognition events between antibodies immobilized on each working electrode and different antigens flowing into the chamber.[25,27,39] In this respect CT represents an ideal test for detection schemes targeting bacterial toxins. Thus, our approach is expected to be easily adapted to other analytes, *e.g.* for the specific detection of multiplex toxins such as ricin, staphylococcal enterotoxin B as done for example by Ligler and other groups.[25,27,39] Another field of application for our biochips could be the early detection of toxins and potential etiological agents (contaminations or bioterrorism agents) in clinical, food and environmental sample. This is an aspect of social importance since this technology would allow also to facilitate prevention by performing routine tests and early detection of infectious agents with epidemic potential.

## Acknowledgements

This work was partially supported by the Italian Institute of Technology (IIT) and by MIUR FIRB Project No. BNE03FMCJ_003.

## References

1 D. Figeys and D. Pinto, *Anal. Chem.*, 2000, **72**, 330A–335A.
2 P. S. Dittrich and A. Manz, *Nat. Rev. Drug Discovery*, 2006, **5**, 210–218.

3 H. Andersson and A. van den Berg, *Sens. Actuators, B*, 2003, **92**, 315–325.
4 V. Srinivasan, V. K. Pamula and R. B. Fair, *Lab Chip*, 2004, **4**, 310–315.
5 J. Wang, M. Pumera, M. P. Chatrathi, A. Escarpa, R. Konrad, A. Griebel, W. Dorner and H. Lowe, *Electrophoresis*, 2002, **23**, 596–601.
6 B. H. Weigl, R. L. Bardell and C. R. Cabrera, *Adv. Drug Delivery Rev.*, 2003, **55**, 349–377.
7 E. Primiceri, M. S. Chiriacò, E. D'Amone, E. Urso, R. E. Ionescu, A. Rizzello, M. Maffia, R. Cingolani, R. Rinaldi and G. Maruccio, *Biosens. Bioelectron.*, 2010, **25**, 2711–2716.
8 G. Walter, K. Bussow, A. Lueking and J. Glokler, *Trends Mol. Med.*, 2002, **8**, 250–253.
9 T. El Hage, C. Merlen, S. Fabrega and F. Authier, *FEBS J.*, 2007, **274**, 2614–2629.
10 M. L. Torgersen, G. Skretting, B. van Deurs and K. Sandvig, *J. Cell Sci.*, 2001, **114**, 3737–3747.
11 C. E. Miller, J. Majewski, R. Faller, S. Satija and T. L. Kuhl, *Biophys. J.*, 2004, **86**, 3700–3708.
12 S. Ahn-Yoon, T. R. DeCory, A. J. Baeumner and R. A. Durst, *Anal. Chem.*, 2003, **75**, 2256–2261.
13 N. Bunyakul, K. A. Edwards, C. Promptmas and A. J. Baeumner, *Anal. Bioanal. Chem.*, 2009, **393**, 177–186.
14 World Health Organization report on global surveillance of epidemic-prone infectious diseases: chapter 4-cholera, http://www.who.int/topics/cholera/surveillance/en/index.html.
15 D. A. Sack, R. B. Sack, G. B. Nair and A. K. Siddique, *Lancet*, 2004, **363**, 223–233.
16 C. A. Rowe-Taitt, J. J. Cras, C. H. Patterson, J. P. Golden and F. S. Ligler, *Anal. Biochem.*, 2000, **281**, 123–133.
17 H. Chen, Y. Zheng, J. H. Jiang, H. L. Wu, G. L. Shen and R. Q. Yu, *Biosens. Bioelectron.*, 2008, **24**, 684–689.
18 K. S. Phillips and Q. Cheng, *Anal. Chem.*, 2005, **77**, 327–334.
19 X. D. Song and B. I. Swanson, *Anal. Chem.*, 1999, **71**, 2097–2107.
20 K. A. Edwards and J. C. March, *Anal. Biochem.*, 2007, **368**, 39–48.
21 S. Kunneke and A. Janshoff, *Angew. Chem., Int. Ed.*, 2002, **41**, 314–316.
22 M. Zayats, O. A. Raitman, V. I. Chegel, A. B. Kharitonov and I. Willner, *Anal. Chem.*, 2002, **74**, 4763–4773.
23 J. C. Miller, H. P. Zhou, J. Kwekel, R. Cavallo, J. Burke, E. B. Butler, B. S. Teh and B. B. Haab, *Proteomics*, 2003, **3**, 56–63.
24 V. C. Rucker, K. L. Havenstrite and A. E. Herr, *Anal. Biochem.*, 2005, **339**, 262–270.
25 J. B. Delehanty and F. S. Ligler, *Anal. Chem.*, 2002, **74**, 5681–5687.
26 M. Labib, M. Hedstrom, M. Amin and B. Mattiasson, *Anal. Chim. Acta*, 2009, **634**, 255–261.
27 W. Lian, D. H. Wu, D. V. Lim and S. G. Jin, *Anal. Biochem.*, 2010, **401**, 271–279.
28 P. T. Charles, F. Velez, C. M. Soto, E. R. Goldman, B. D. Martin, R. I. Ray and C. R. Taitt, *Anal. Chim. Acta*, 2006, **578**, 2–10.
29 C. L. Schofield, R. A. Field and D. A. Russell, *Anal. Chem.*, 2007, **79**, 1356–1361.
30 X. L. Luo, A. Morrin, A. J. Killard and M. R. Smyth, *Electroanalysis*, 2006, **18**, 319–326.
31 S. Loyprasert, M. Hedstrom, P. Thavarungkul, P. Kanatharana and B. Mattiasson, *Biosens. Bioelectron.*, 2010, **25**, 1977–1983.
32 C. Gondran, M. Orio, D. Rigal, B. Galland, L. Bouffier, T. Gulon and S. Cosnier, *Electrochem. Commun.*, 2010, **12**, 311–314.
33 S. Viswanathan, L. C. Wu, M. R. Huang and J. A. A. Ho, *Anal. Chem.*, 2006, **78**, 1115–1121.
34 E. Katz and I. Willner, *Electroanalysis*, 2003, **15**, 913–947.
35 A. J. Bard and L. R. Faulkner, *Electrochemical Methods: Fundamentals and Applications*, Wiley, New York, 1980.
36 L. Yang and Y. Li, *Biosens. Bioelectron.*, 2005, **20**, 1407–1416.
37 S. L. Pan and L. Rothberg, *Langmuir*, 2005, **21**, 1022–1027.
38 G. Maruccio, E. Primiceri, P. Marzo, V. Arima, A. Della Torre, R. Rinaldi, T. Pellegrino, R. Krahne and R. Cingolani, *Analyst*, 2009, **134**, 2458–2461.
39 C. R. Taitt, G. P. Anderson, B. M. Lingerfelt, M. J. Feldstein and F. S. Ligler, *Anal. Chem.*, 2002, **74**, 6114–6120.
40 Q. Cheng, S. M. Zhu, J. Song and N. Zhang, *Analyst*, 2004, **129**, 309–314.
41 M. M. Ngundi, C. R. Taitt and F. S. Ligler, *Biosens. Bioelectron.*, 2006, **22**, 124–130.


 